25th ABCM International Congress of Mechanical Engineering
October 20-25, 2019, Uberlândia, MG, Brazil

COB-2019-1212
A Transient Model for Estimating APB in Short Time Operations

Ianto Oliveira Martins
Arthur Pandolfo da Veiga
Eduardo Bader Dalfovo Mohr Alves
Alexandre Kupka da Silva
Jader Riso Barbosa Jr
Departamento de Engenharia Mecânica
Universidade Federal de Santa Catarina
ianto.oliveira@polo.ufsc.br
arthur.veiga@polo.ufsc.br
eduardo.alves@polo.ufsc.br
a.kupka@ufsc.br
jrb@polo.ufsc.br

Abstract: *A transient heat transfer model based on a literature work is used to simulate the heat transfer on an offshore well. This model consists on separating the well as a sequence of layers, e.g. injection fluid, tubing, annular and casing. Each layer is modeled 1D axially and exchanges heat with adjacent layers through a thermal resistance method, which considers the annular fluids static. The results indicate the injection fluid enters steady state after 1 h. After 6 h, Annular A exchanges more energy with the injection fluid than the others, reaching a steady state. Annular B and C maintain a temperature profile close to the one from the rock formation, due to their proximity. APB was calculated for 6 h time, with Annular B achieving the higher absolute value, highlighting the importance of studying the APB behavior for injection operations also.*

Keywords: *APB, Transient model, Heat transfer, Injection well*

1. INTRODUCTION

Development of more advanced technologies in recent years enabled petroleum exploration on deepwater reservoirs. These reservoirs are known for high pressure and temperature operation conditions. These conditions require special planning and design to avoid accidents.

Annular Pressure Buildup (APB) is inevitable when there is heat transfer in the wellbore, causing annular fluid to increase or reduce its volume, which may lead to a loss of the well structural integrity (Moe and Erpelding, 2000). APB has already been reported as the responsible for some documented accidents (Bradford *et al.*, 2004). Oudeman and Kerem (2004) considers three factors on the APB calculation: annular fluid thermal expansion, casing deformation and fluid leakoff. These terms are presented in Eq. (1).

$$\Delta p = \left(\frac{\partial p}{\partial m}\right)_{V_{an},T} \Delta m + \left(\frac{\partial p}{\partial V_{an}}\right)_{m,T} \Delta V_{an} + \left(\frac{\partial p}{\partial T}\right)_{V_{an},m} \Delta T \tag{1}$$

In Eq. (1), p is pressure, m is the fluid mass in the annular, V_{an} is the volume occupied by the annular fluid and T is temperature. In the right hand side of the equation, the first term is pressure variation due to the mass outlet or inlet at the annular, the second term is the pressure variation due to the casing deformation and the third term is the pressure change due to the effect of expansion or compression. According to Hasan *et al.* (2010), the third term accounts for more than 80% of the total APB.

APB studies, so far, are only concerned with production operations, when the annuli fluid are heated and, consequently, expand and the internal pressure rises. On the other hand, injection operations may involve a different set of phenomena, while there are operations involving saturated steam injection (Sun *et al.*, 2018), cold fluid injection are more common. As consequence, the well is cooled, and the annulus internal pressure is reduced.

On the heat and momentum transfer in the well, earliest studies date back to Ramey (1962), which considered a single phase injection on a well, with steady state heat and momentum transfer in the well, and transient heat transfer with the adjacent rock formation. To model this transient heat transfer, a dimensionless time function was used to calculate the temperature at the interface between well and formation. Later works sought to improve on this method and developed new time functions. Both Chiu and Thakur (1991) and Hasan and Kabir (1991) developed time funcions to consider the effect of heat transfer in shorter times of operation, usually less than 7 days. Cheng *et al.* (2011) considered the effect the formation thermophysical properties have on the formation temperature profile. Ferreira *et al.* (2017) developed a hybrid time function, comprised of previously published models, to cover a larger time range.

More recently, Yi *et al.* (2018) developed a transient model to simulate the injection of supercritical carbon dioxide on an offshore well. This model calculates the temperature profile at every vertical layer of the well.

For production operations, technical staff are mainly concerned with longer-time operations, when problems involving APB arise, and most models present in the literature, analytical and numerical, present adequate results for longer-time but do not for shorter-time operations (Tang *et al.*, 2019), reinforcing the need for transient models.

This work seeks to improve on Yi *et al.* (2018) work, being able to calculate the APB over time and also considering the variation of thermophysical properties of the injection and annular fluids with the commercial software Multiflash (Infochem/KBC, 2018). The discretization of the equations was performed with finite difference method and its implementation and solving was on Python (Foundation, 2019). The geometry of the simulated well comes from a past work in the group (Barcelos, 2017), which modeled the APB for production operations.

2. MATHEMATICAL MODEL

The mathematical model consists on a force and energy balance on a control volume. The model is 1D steady for the force balance and 1D transient for the heat transfer. The radial heat transfer, with the adjacent layers considers a thermal resistance network, and all the fluids at the well, other than the injection fluid, are considered static. The energy balance is made as function of temperature and considers the Joule-Thomson effect. Wellbores are commonly simulated as a set of concentric cylinders, as seen in Figure 1.

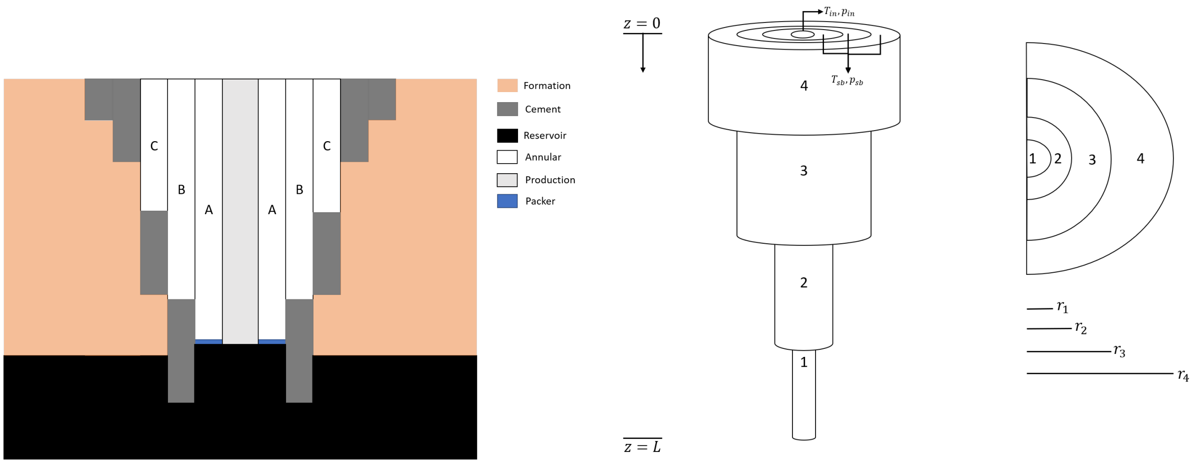

(a) Wellbore sketch (b) Concentric cylinder view

Figure 1. Wellbore sketch

Eq. (2) calculates the injection fluid pressure, Eq. (3) calculates the annuli fluid pressure and Eq. (4) calculates the friction factor for single phase flow. In these equations ρ_1 is the injection fluid density, θ is the well inclination angle, v is the injection fluid velocity, r_1 is the tubing radius, f is the friction factor (Colebrook *et al.*, 1939), K is the tubing rugosity, Re is the Reynolds number associated to the injection fluid flow, μ_1 is the injection fluid viscosity.

$$\frac{dp_1}{dz} = \rho_1 g \sin\theta - f\frac{\rho_1 v^2}{4r_1} - \rho_1 v_1 \frac{dv_1}{dz} \tag{2}$$

$$\frac{dp_i}{dz} = \rho_i g \tag{3}$$

$$\frac{1}{\sqrt{f}} = -2\log\left(\frac{K}{7.4r_1} + \frac{2.51}{\mathrm{Re}\sqrt{f}}\right) \tag{4}$$

$$\mathrm{Re} = \frac{2\rho_1 v_1 r_1}{\mu_1} \tag{5}$$

The energy balance was performed on each layer of the wellbore: it considered the enthalpy flow on the control volume boundaries, the internal energy variation through time, the in and outward radial heat transfer on each layer and the viscous dissipation of the injection fluid. The subscript of each variable indicates the layer on which the calculation is being performed.

Eqs. (6) and (7) refer to the first and second layers, whereas the remaining layers energy balance equations may be generalized and are represented by Eqs. (8) and (9), the latter representing liquid layers and the former the solid layers. Remaining terms are calculated by Eqs. (10) and (11). On these equations c_p is the specific heat, h_1 is the convective heat transfer coefficient (Dittus and Boelter, 1985), $\mu(T_2)$ is the viscosity evaluated at the second layer temperature, Q_1 is the viscous dissipation, α_J is the Joule-Thomson coefficient, k is the equivalent thermal conductivity of the layer, $\left(\frac{dp_1}{dz}\right)_{fr}$ is the frictional pressure drop gradient, described by the second term of Equation (2), q is the inlet fluid flow rate, Ra is the Rayleigh number, Pr is the Prandtl number.

$$\rho_1 c_{p_1}\frac{\partial T_1}{\partial t} + \rho_1 v_1 c_{p_1}\frac{\partial T_1}{\partial z} - \frac{2h(T_2 - T_1)}{r_1} = (1 + \alpha_J \rho_1 c_{p_1})\left(\frac{\partial p_1}{\partial t} + v_1\frac{\partial p_1}{\partial z}\right) + \frac{Q_1}{\pi r_1^2} \tag{6}$$

$$\rho_2 c_{p_2}\frac{\partial T_2}{\partial t} - \frac{2k_2k_3(T_3 - T_2)}{\left(k_3 \ln\frac{2r_2}{r_1+r_2} + k_2\ln\frac{r_3+r_2}{2r_2}\right)(r_2^2 - r_1^2)} + \frac{2r_1h(T_2 - T_1)}{r_2^2 - r_1^2} - \frac{\partial}{\partial z}\left(k_2\frac{\partial T_2}{\partial z}\right) = 0 \tag{7}$$

$$\rho_i c_{p_i}\frac{\partial T_i}{\partial t} - \frac{2k_ik_{i+1}(T_{i+1} - T_i)}{\left(k_{i+1}\ln\frac{2r_i}{r_i+r_{i-1}} + k_i\ln\frac{r_i+r_{i+1}}{2r_i}\right)(r_i^2 - r_{i-1}^2)} + \frac{2k_ik_{i-1}(T_i - T_{i-1})}{\left(k_i\ln\frac{2r_{i-1}}{r_{i-1}+r_{i-2}} + k_{i-1}\ln\frac{r_{i-1}+r_i}{2r_{i-1}}\right)(r_i^2 - r_{i-1}^2)} - \frac{\partial}{\partial z}\left(k_i\frac{\partial T_i}{\partial z}\right) = 0 \tag{8}$$

$$\rho_i c_{p_i}\frac{\partial T_i}{\partial t} - \frac{2k_ik_{i+1}(T_{i+1} - T_i)}{\left(k_{i+1}\ln\frac{2r_i}{r_i+r_{i-1}} + k_i\ln\frac{r_i+r_{i+1}}{2r_i}\right)(r_i^2 - r_{i-1}^2)} + \frac{2k_ik_{i-1}(T_i - T_{i-1})}{\left(k_i\ln\frac{2r_{i-1}}{r_{i-1}+r_{i-2}} + k_{i-1}\ln\frac{r_{i-1}+r_i}{2r_{i-1}}\right)(r_i^2 - r_{i-1}^2)} - \frac{\partial}{\partial z}\left(k_i\frac{\partial T_i}{\partial z}\right) = (1 + \rho_i\alpha_J c_{p_1})\frac{\partial p_i}{\partial t} \tag{9}$$

$$h_1 = 0.0115\left(\frac{k_1}{r_1}\right)\mathrm{Re}_1^{0.8}\mathrm{Pr}_1^{1/3}\left(\frac{\mu_1}{\mu_1(T_2)}\right)^{0.14} \tag{10}$$

$$Q_1 = q\left(\frac{dp_1}{dz}\right)_{fr} \tag{11}$$

It is possible to consider the natural convection effect inside the annuli by using an appropriate correlation. The correlation used in this work is described by Eq. (12) (Zhou, 2013).

$$k_{eq} = \begin{cases} k_i & \mathrm{Ra} \leq 6\cdot 10^3 \\ 0.13k_i\mathrm{Ra}^{0.25} & 6\cdot 10^3 < \mathrm{Ra} \leq 5\cdot 10^5 \\ 0.049k_i\mathrm{Ra}^{1/3}\mathrm{Pr}^{0.074} & 5\cdot 10^5 < \mathrm{Ra} \leq 7.18\cdot 10^8 \end{cases} \tag{12}$$

$$\mathrm{Ra} = \frac{\rho g\beta c_p\Delta T\Delta r^3}{\mu k} \tag{13}$$

The APB was calculated by Eq. (14), considering only the thermal parcel of Eq. (1). In this equation, β is the fluid thermal expansivity coefficient and κ is the fluid compressibility coefficient. It was considered the average value at each time step for the whole fluid column.

$$\Delta p_i = \frac{1}{L}\int_0^L \frac{\beta_i}{\kappa_i}\Delta T_i \mathrm{d}z \tag{14}$$

For the force balance, the initial pressure profile on all the layers are hydrostatic, and the pressure on the inlet is prescribed. For the energy balance, all the layers are on thermal equilibrium with the adjacent formation, the inlet temperature is the same as the seabed and the outlet of all layers, except the injection fluid one, is considered adiabatic.

Heat transfer between the injection fluid and the adjacent formation is represented by Eqs. (15) and (16). In Eq. (15), r_{wb} is the outer radius of the well, U_{wb} is the wellbore global heat transfer coefficient and T_f is the formation temperature. Eq. (16) shows how the calculation of U_{wb} is performed, it is the summatory of all thermal resistances inside the well, up to the formation, as shown by the summatory upper index f.

$$Q = -2\pi r_{wb}U_{wb}\left(T - T_f\right) \tag{15}$$

$$U_{wb} = \left(\frac{r_2}{r_1 h_1} + \sum_{i=2}^{f}\frac{r_i}{k_i}\ln\left(\frac{r_i}{r_{i-1}}\right)\right)^{-1} \tag{16}$$

Previous works simulated long operation times and used dimensionless time functions to estimate the temperature at the interface between well and formation. Since the present work will simulate a short time transient operation, the interfacial temperature between formation and well will remain constant through the simulation.

Figure 2 presents a schematic of the simulated wellbore. Injection pressure was 55 MPa, injection flowrate was 0.066 m^3 s^{-1}, seabed temperature was 277.15 K and its height was 1387 m. Simulation was performed up to the point of the PDG sensor, so the simulated tubing height was 2503 m. Annular A was formed by gaseous N_2, Annular B and C were modeled as a mixture between glycol and water 50/50 % mass and the injection fluid was brine, with 27 % mass of salt. The well is vertical, i.e. $\theta = 90^o$ throughout its depth.

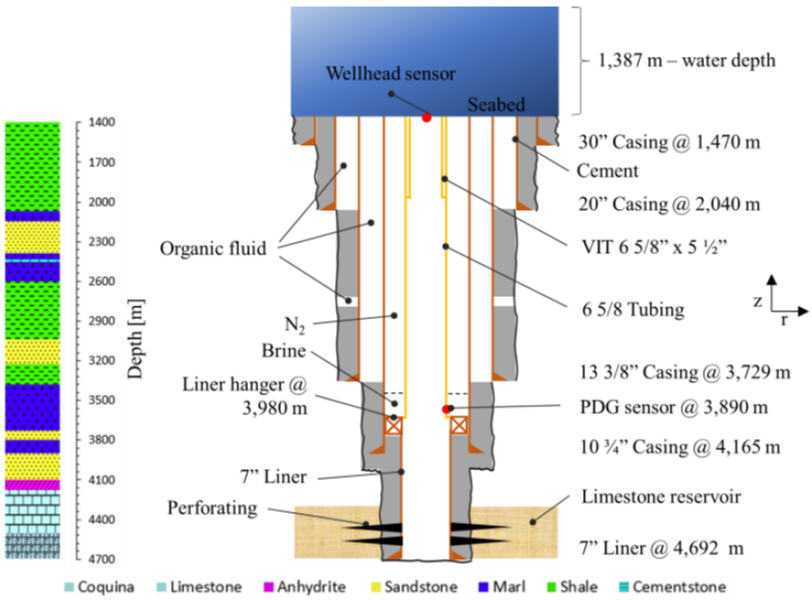

Figure 2. Simulated well schematic (Ferreira, 2017)

The mesh used in the simulation is described by Figure 3. Note that while in the axial direction the number of control volumes depends on the mesh refinement, the number of nodes on the radial direction depends on the well configuration, i.e. the number of layers. The simulated well contain 11 layers, with three of them being the annuli fluids and one the injection fluid.

Figure 3 also contains the boundary conditions used in the simulation. For the static layers, two boundary conditions are needed: prescribed temperature at the inlet and no-flux at the bottom were chosen due to being physically adequate and also increases the model numerical stability. In the simulation performed, there were 300 control volumes on each layer and the time step was 60 s.

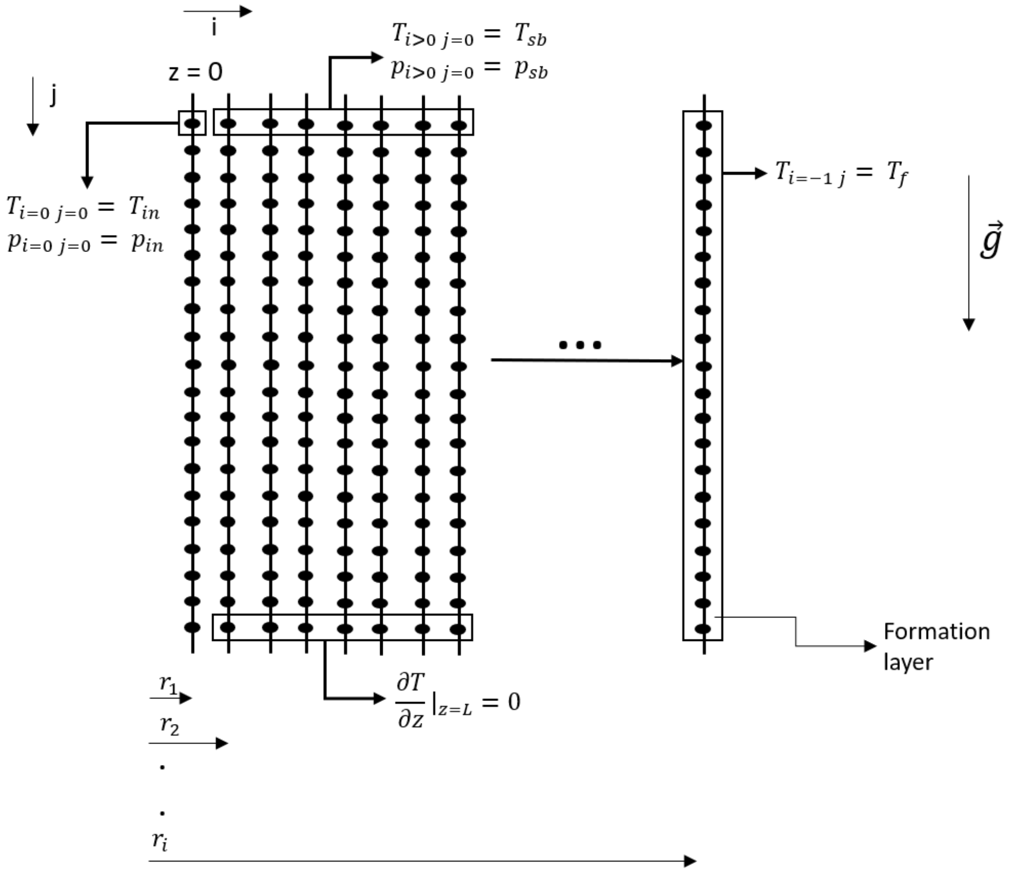

Figure 3. Mesh used in the simulation

3. RESULTS

Figures 4, 5, 6 and 7 present the pressure profiles after 1 hour of operation for the fluid layers of the well. The choice for this time range is so the variation on the annular pressure profiles is more perceptible. While the pressure profile of the injection fluid presents no visible variation, more perceptible variations are present for the annuli, mainly due to the APB effect, which will be also discussed in this work.

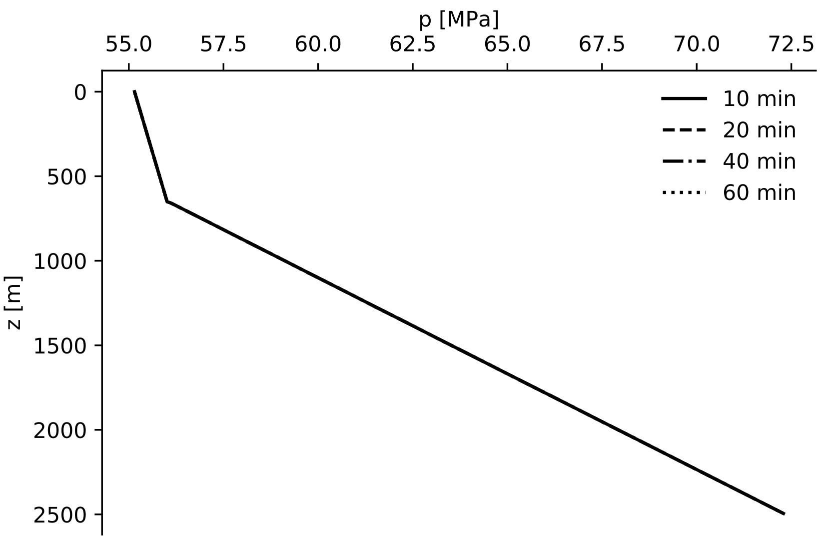

Figure 4. Injection fluid pressure profile

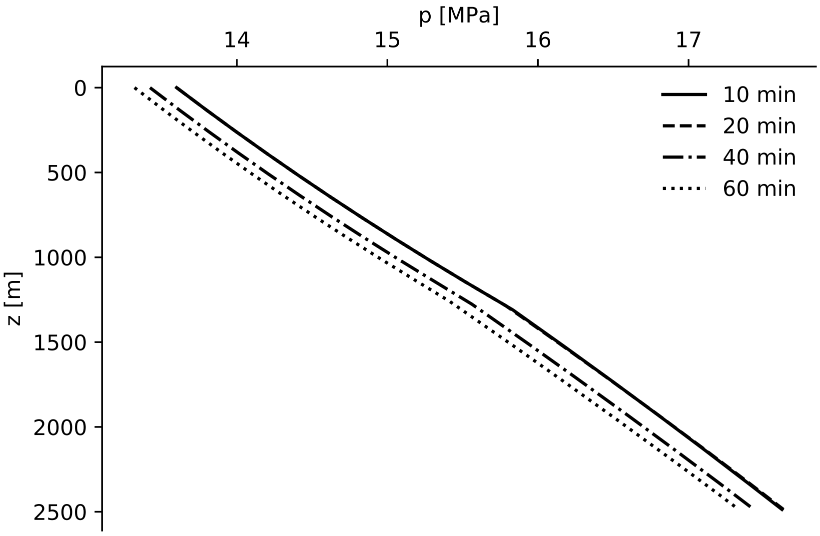

Figure 5. Annular A fluid pressure profile

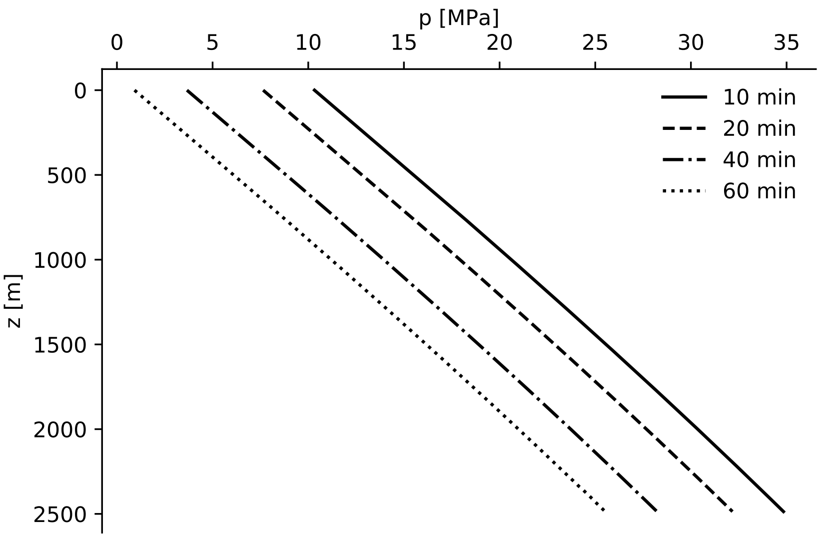

Figure 6. Annular B fluid pressure profile

Figures 8 and 9 present the injection fluid temperature profile throughout the operation. The initial temperature profile of all the wellbore layers was the same as the formation. The injection fluid temperature profile quickly reaches a state close to a steady state, as further shown in Figure 9. This can be explained by the high thermal inertia of the injection fluid flow, dominated by the advection mechanism.

Figures 10, 11, 12 and 13 show the annuli temperature profile at different operation times. For comparative purposes, the formation temperature profile was also plot on these figures. It is possible to see the effect of the injection fluid high thermal inertia combined to the Annular A fluid, gaseous N_2, reduced thermal conductivity: the temperature of annuli B and C change very little in comparison to their initial temperature profile.

Figure 14 shows the heat transfer per unit length for 4 different times: 1, 2, 4 and 6 h. From this image it can be seen that heat transfer profile presents no significant changes over time, it can be explained by two different factors, the first one being that after one hour the temperature difference between the injection fluid and the formation temperature profile presents no variation, as can be seen in Figure 9. The second would be the reduced variation the fluids layers' thermal conductivities present over time, resulting in a reduced global heat transfer coefficient, described by Eq. (16).

The discontinuities present in Figure 14 are inherent to the process, due to the well geometry, such results are found on other works in the literature (Ferreira, 2017; Barcelos, 2017). In these works it is also possible to see these discontinuities

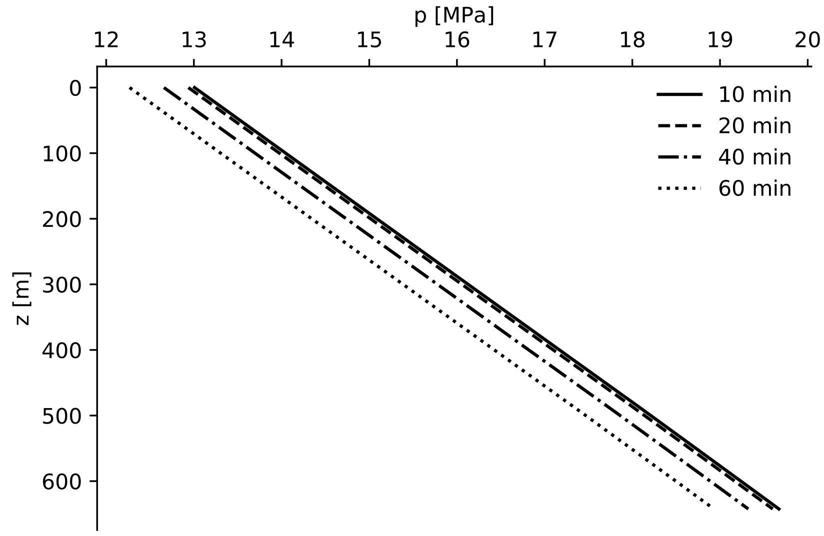

Figure 7. Annular C fluid pressure profile

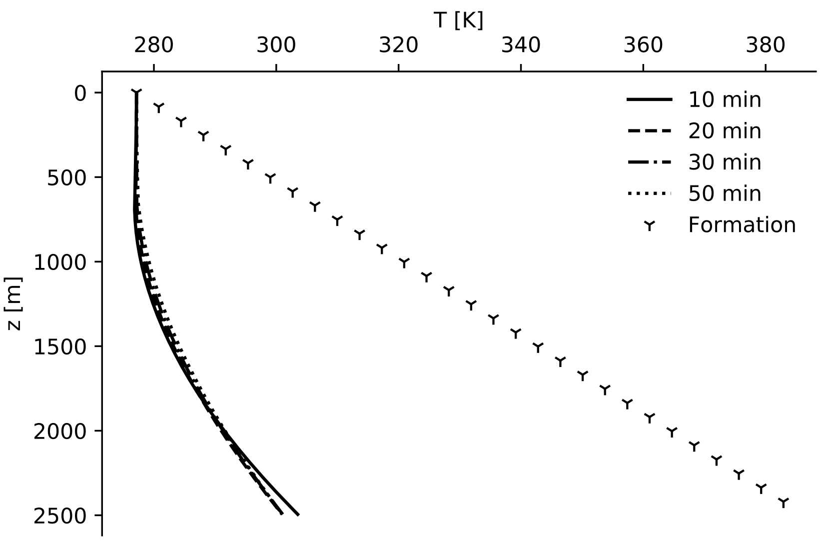

Figure 8. Injection fluid temperature before 1 h

on temperature and pressure profiles, but contrary to the present work, these ones simulate production operations.

Figure 15 shows the APB after 6 h of operation. The APB calculated here is negative because this process involves the cooling of the well, via injection of a cold fluid. This cooling implies reducing all the layers temperatures, including the annular ones, and with this temperature reducing, an attempt at compression of the fluid occurs. Despite presenting higher values for the temperature difference through time, Annular A APB is lower compared to the other annuli due to the lower gaseous N_2 isothermal compressibility.

While the positive APB values raise concerns due to the possibility of casing collapse, negative values of APB are also damaging to a well due to a potential loss of structural stability, consequence of losing the original balance of forces from when drilling the well.

4. CONCLUSION

A transient heat transfer model was adapted to simulate the heat transfer on wellbores, being able to estimate the APB over time. Currently, few studies contemplate transient heat transfer models for wellbore operations and even fewer works consider injection operations on the simulations.

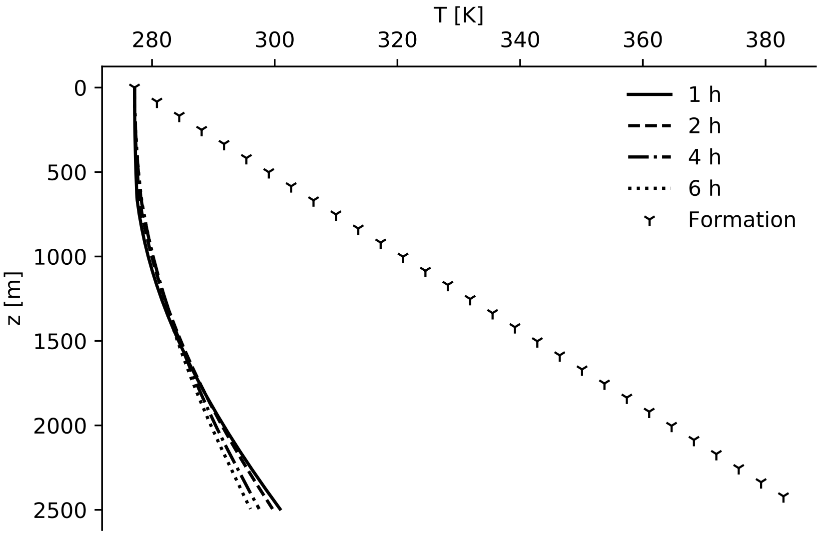

Figure 9. Injection fluid temperature after 1 h

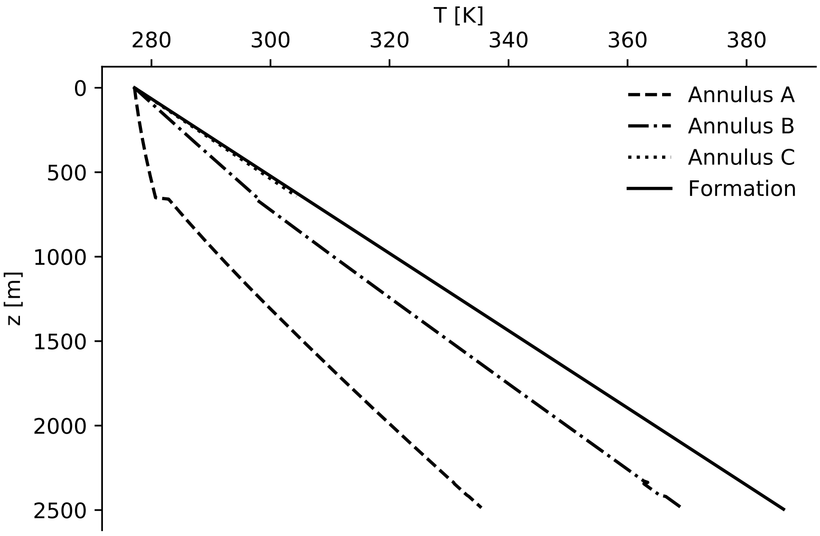

Figure 10. Annuli temperature profile at 1 h of injection

The wellbore here simulated was originally studied for a long-time production operation, which achieved values as high as 80 MPa. This study demonstrates how APB is also present for injection operations and needs to be taken into account when designing this class of wellbores.

The present model can be used in the simulation of other operations and geometries by only changing its boundary conditions, and wellbore specifications. It advances on the current literature by considering thermophysical properties variation in all fluid layers and by computing the thermal APB. Future versions of the model will also include the APB parcels of structural deformation and fluid leakoff.

5. ACKNOWLEDGEMENTS

The authors would like to acknowledge both CNPq and Petrobras for the financial support.

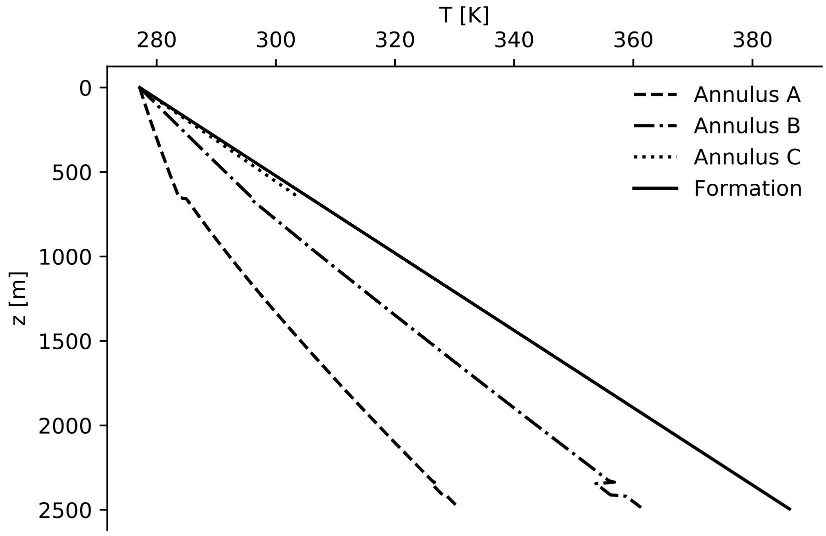

Figure 11. Annuli temperature profile at 2 h of injection

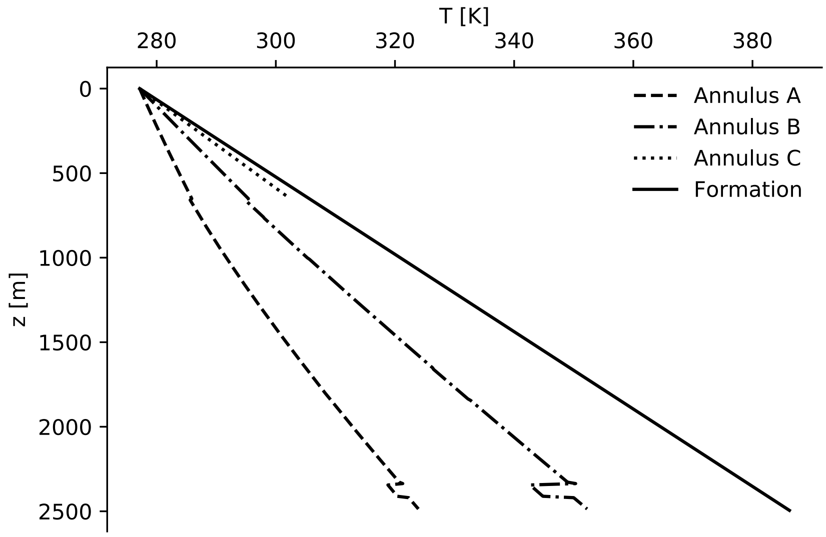

Figure 12. Annuli temperature profile at 4 h of injection

6. REFERENCES

Barcelos, J.G.A., 2017. *Modelagem Matemática do Aumento de Pressão nos Anulares (APB) em PoÃğos de Petróleo (in portuguese)*. Master's thesis, Department of Mechanical Engineering, Federal University of Santa Catarina, Florianópolis.

Bradford, D., Fritchie Jr, D., Gibson, D., Gosch, S., Pattillo, P., Sharp, J. and Taylor, C., 2004. "Marlin failure analysis and redesign: part 1-description of failure". *SPE Drilling & Completion*, Vol. 19, No. 02, pp. 104–111.

Cheng, W.L., Huang, Y.H., Lu, D.T. and Yin, H.R., 2011. "A novel analytical transient heat-conduction time function for heat transfer in steam injection wells considering the wellbore heat capacity". *Energy*, Vol. 36, No. 7, pp. 4080–4088.

Chiu, K. and Thakur, S., 1991. "Modeling of wellbore heat losses in directional wells under changing injection conditions." In *SPE Annual Technical Conference and Exhibition*. Society of Petroleum Engineers.

Colebrook, C.F., Blench, T., Chatley, H., Essex, E., Finniecome, J., Lacey, G., Williamson, J. and Macdonald, G., 1939. "Correspondence. turbulent flow in pipes, with particular reference to the transition region between the smooth and rough pipe laws.(includes plates)." *Journal of the Institution of Civil engineers*, Vol. 12, No. 8, pp. 393–422.

Dittus, F. and Boelter, L., 1985. "Heat transfer in automobile radiators of the tubular type". *International Communications*

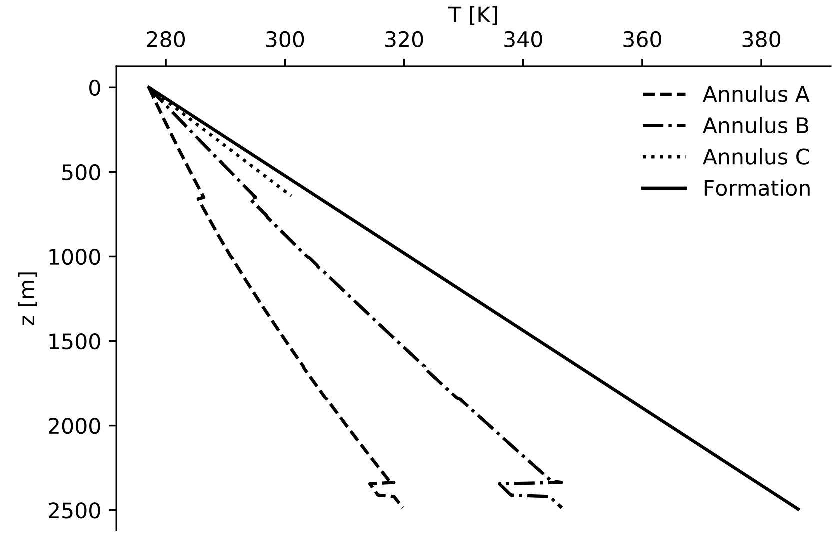

Figure 13. Annuli temperature profile at 6 h of injection

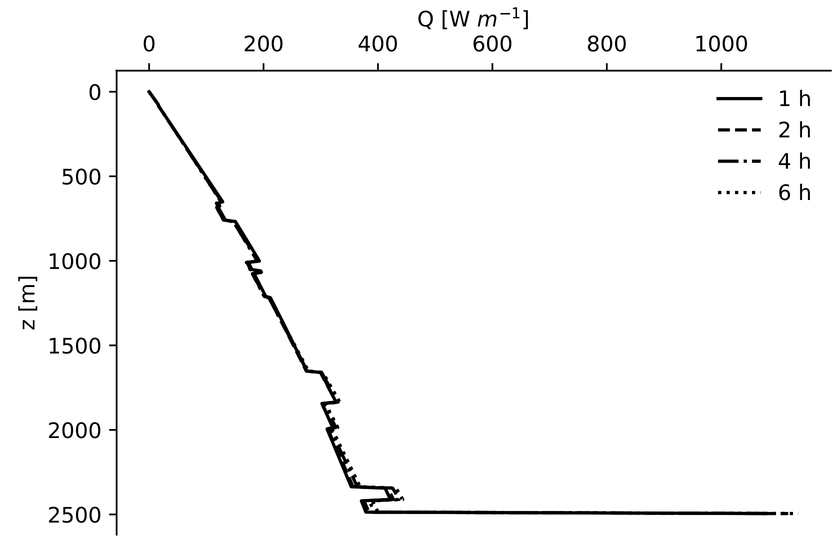

Figure 14. Heat transfer per unit length

in Heat and Mass Transfer, Vol. 12, No. 1, pp. 3–22.

Ferreira, M.V., Hafemann, T.E., Barbosa Jr, J.R., da Silva, A.K. and Hasan, R., 2017. "A numerical study on the thermal behavior of wellbores". *SPE Production & Operations*, Vol. 32, No. 04, pp. 564–574.

Ferreira, M.V.D., 2017. *THERMAL-STRUCTURAL STUDY OF WELLBORES WITH VACUUM INSULATED TUBINGS*. Ph.D. thesis, Department of Mechanical Engineering, Federal University of Santa Catarina, Florianópolis.

Foundation, P.S., 2019. "Python 3.8.0a2 documentation". URL `https://docs.python.org/3.8/`. Accessed: 2019-03-25.

Hasan, A. and Kabir, C., 1991. "Heat transfer during two-phase flow in wellbores; part i–formation temperature". In *SPE Annual Technical Conference and Exhibition*. Society of Petroleum Engineers.

Hasan, R., Izgec, B. and Kabir, S., 2010. "Sustaining production by managing annular-pressure buildup". *SPE Production & Operations*, Vol. 25, No. 02, pp. 195–203.

Infochem/KBC, 2018. "Multiflash^{TM} v7.0." URL `https://www.kbc.global/`. Accessed: 2019-01-30.

Moe, B. and Erpelding, P., 2000. "Annular pressure buildup: What it is and what to do about it." *World Oil*, Vol. 221, No. 8, pp. 21–23.

Oudeman, P. and Kerem, M., 2004. "Transient behavior of annular pressure build-up in hp/ht wells". *SPE Drilling &*

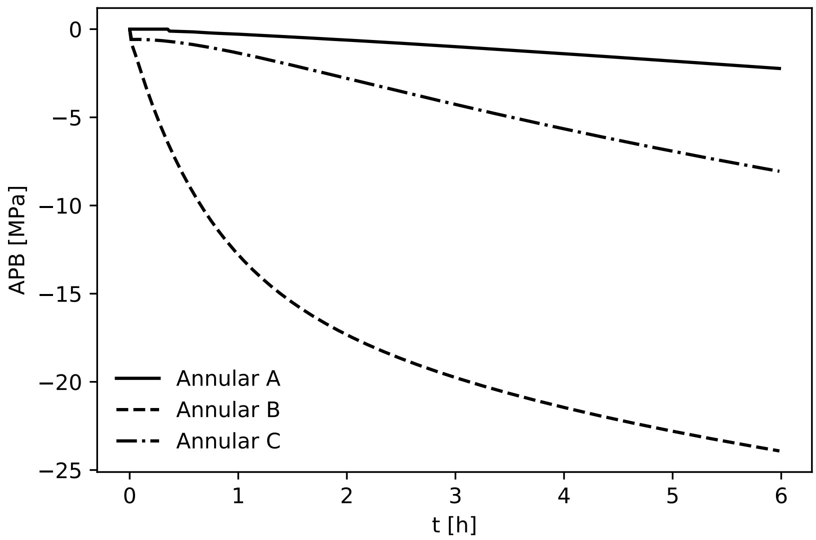

Figure 15. Annular pressure buildup

Completion, Vol. 21, No. 04, pp. 234–241.

Ramey, H., 1962. "Wellbore heat transmission". *Journal of Petroleum Technology*, Vol. 14, No. 04, pp. 427–435.

Sun, F., Yao, Y., Li, X., Li, G. and Sun, Z., 2018. "A numerical model for predicting distributions of pressure and temperature of superheated steam in multi-point injection horizontal wells". *International Journal of Heat and Mass Transfer*, Vol. 121, pp. 282–289.

Tang, H., Xu, B., Hasan, A.R., Sun, Z. and Killough, J., 2019. "Modeling wellbore heat exchangers: Fully numerical to fully analytical solutions". *Renewable Energy*, Vol. 133, pp. 1124–1135.

Yi, L.P., Li, X.G., Yang, Z.Z. and Sun, J., 2018. "Coupled calculation model for transient temperature and pressure of carbon dioxide injection well". *International Journal of Heat and Mass Transfer*, Vol. 121, pp. 680 – 690. ISSN 0017-9310. doi:https://doi.org/10.1016/j.ijheatmasstransfer.2018.01.036.

Zhou, F., 2013. "Research on heat transfer in geothermal wellbore and surroundings".

7. RESPONSIBILITY NOTICE

The authors are the only responsible for the printed material included in this paper.